Available online at www.sciencedirect.com
SCIENCE DIRECT®
Carbohydrate Research 340 (2005) 2520–2532
Carbohydrate RESEARCH

Conformational folding of xyloglucan side chains in aqueous solution from molecular dynamics simulation

Myco Umemura[a] and Yoshiaki Yuguchi[b,*]

[a]*Graduate School of Biostudies, Kyoto University, Division of Integrated Life Science, Oiwake-cho, Kitashirakawa, Sakyo-ku, Kyoto 606-8502, Japan*
[b]*National Institute of Advanced Industrial Science and Technology, AIST, 2266-98 Anagahora, Shimoshidami, Moriyama-ku, Nagoya-shi, Aichi 463-8560, Japan*

Received 19 July 2005; accepted 22 August 2005
Available online 5 October 2005

Abstract—Molecular dynamics simulation was carried out on xyloglucan with explicit water molecules to investigate the folding mechanism of side chains onto a main chain in aqueous solution. The model xyloglucan was composed of 12 β-D-glucopyranoses as a main chain substituted with six galactoses and three xyloses as side chains. Two conditions were set for the ribbon-like main chain; one is restricted to be 'flat' and the other is without restriction. The free main chain of xyloglucan has a 'twisted' conformation as the major one. Conformational folding of side chains onto the main chain was analyzed with dihedral angles at each glycosidic linkage. In a 5-ns calculation, the xyloglucan has a tendency to contract in both the restricted and the free systems, but the mode of contraction is different. Side chains tend to stick onto the flat surface of the main chain in the restricted system, while they do not tightly do so in the free one; instead the main chain takes a twisted and sometimes embowed conformation. This result indicates that the main chain has greater attractive forces to bind side chains when it is flat, while it loses the ability as it is twisted.

Keywords: Xyloglucan; Conformational folding; Dihedral angle; Aqueous solution; Molecular dynamics simulation

1. Introduction

Xyloglucan is a hemicellulosic polysaccharide that is found in the primary cell walls of all higher plants.[1,2] It binds with a strong affinity to cellulosic cell walls, having an important role in cell-wall enlargement.[3,4] It consists of a β-(1→4)-linked glycosyl main chain substituted at O-6 with side chains composed of α-(1→6)-xyloses, β-(1→2)-galactoses, and sometimes α-(1→2)-fucoses. The main chain is identical to the cellulose chain, which has ribbon-like conformation composed of each glycosidic ring face. Although it has a cellulose backbone, it dissolves in water unlike cellulose. Dissolved xyloglucan in aqueous solution can form a gel under certain conditions such as addition of alcohols[5,6] and undergoing enzymatic degradation with β-galactosidase.[7] This means that xyloglucan has both hydrophobic and hydrophilic aspects, one of which can be dominant depending on conditions.

Determination of the conformation of xyloglucan at the atomic level is difficult because branched polysaccharides are not easily crystallized. The experimental data from X-ray fiber diffraction (*Tamarindus indica*[8] and *pea*[9] xyloglucan) have indicated a twofold helical conformation for the main chain in the crystalline state, which is similar to the 'flat' ribbon-like conformation of cellulose chains in the crystal. The main-chain conformation in solution has not been experimentally determined except in a study by Picard et al.[10] They reported a twisted main-chain conformation of xyloglucan heptamer in aqueous solution from NMR and molecular mechanics studies. Their study has revealed that the twisted conformation is significantly populated in solution, although the main chain includes only four glucose residues. A twisted conformation of the main chain is derived from the global minimum conformation

* Corresponding author. Tel.: +81 52 736 7484; fax: +81 52 736 7406; e-mail: y-yuguchi@aist.go.jp

0008-6215/$ - see front matter © 2005 Elsevier Ltd. All rights reserved.
doi:10.1016/j.carres.2005.08.017

of cellobiose.[8,11,12] Sugiyama et al. also reported helical conformations of cellulose oligomers in aqueous solution from an NMR study, although the helical pitches are more moderate than the theoretical one of cellobiose.[13] The orientation of xyloglucan side chains in aqueous solution has not been experimentally deduced with the exception of the report mentioned by Picard et al.[10] The xyloglucan heptamer in their study has only xylose side chains, while most xyloglucans in plants include not only xyloses, but also galactoses and fucoses. Computer simulations such as molecular mechanics[9,10] and Monte Carlo methods[14,15] have been used to investigate the side-chain conformation, but without water.

In this work, we perform molecular dynamics (MD) simulations for a xyloglucan oligomer immersed in explicit water molecules to investigate the mechanism of side-chain folding onto the main chain in aqueous solution. Because there is no evidence for the main-chain conformation in aqueous solution, we set two conditions for it; one is restricted as 'flat' like crystalline cellulose, and the other is without restriction. The main purpose of this work is to compare the difference of folding mechanism between the two main-chain conditions. Although Levy et al. also compared the folding mechanism between flat and twisted main chains,[14] their research attention is on the folding side of one fucosylated side chain on their flat and twisted main chains that are restricted. Their model is composed of nine glucoses as a main chain and five xyloses and one fucosylgalactose as side chains. In addition, they performed the calculation without water. We use a xyloglucan model with 12 glucose residues as a main chain and six galactose and three xylose residues as side chains. We carry out MD calculations under the two conditions of the main chain for 5 ns to obtain enough information about position and momentum of each atom. We analyze the conformational folding of side chains using dihedral angles at each glycosidic linkage, which angles can accurately describe saccharide conformations. Interactions between the main and side chains are discussed with analysis of intramolecular hydrogen bonds.

2. Experimental

2.1. Simulation procedures

The composition of xyloglucan oligomer used in this study is shown in Figure 1 with names and numbering of glycosidic linkages. The main chain is composed of

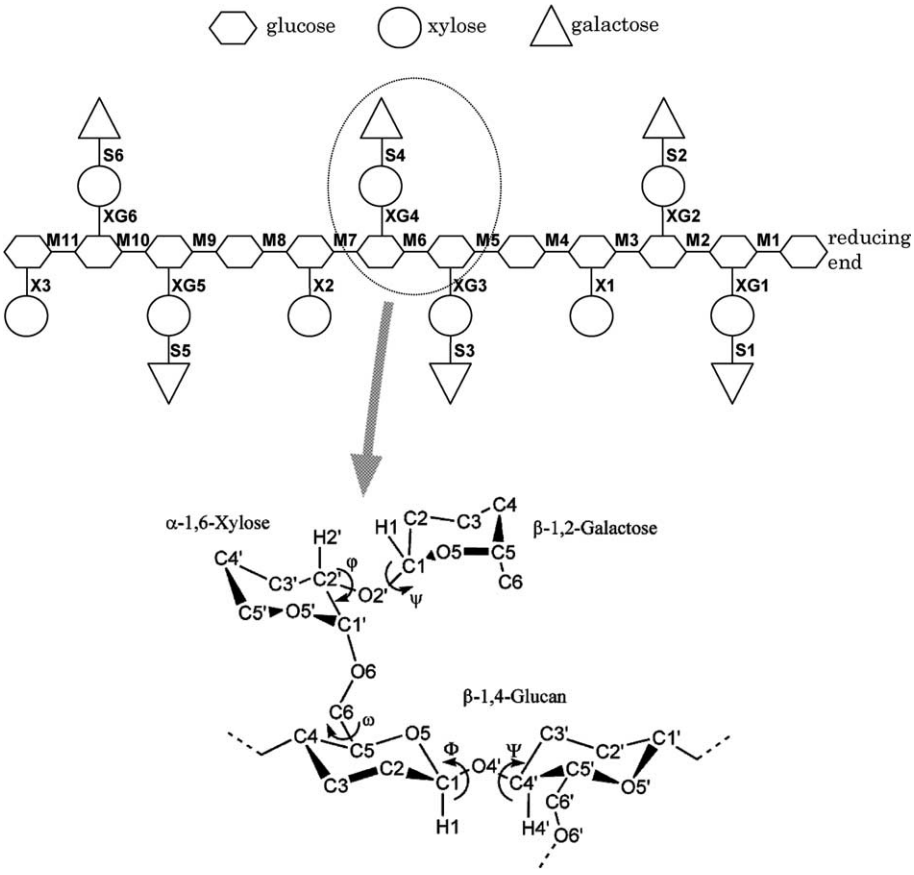

Figure 1. Sequence of xyloglucan used in calculations with names and numbering of glycosidic linkages (above), and definition of dihedral angles Φ, Ψ, ϕ, ψ, and ω (below). Φ = H-1–C-1–O-4′–C-4′, Ψ = C-1–O-4′–C-4′–H-4′, ϕ = H-1–C-1–O-2′–C-2′, ψ = C-1–O-2′–C-2′–H-2′, and ω = O-5–C-5–C-6–O-6.

12 D-glucopyranoses that are connected by β-(1→4)-linkages with each other. The side chains are composed of six galactoxylose and three xylose residues. Xyloses and galactoses are attached to glucoses and xyloses by α-(1→6)- and β-(1→2)-linkages, respectively. The position and the ratio between glucose, xylose, and galactose residues are determined based on previous reports about xyloglucans found in *T. indica*.[16–18] As described in Figure 1, dihedral angles are defined as Φ = H-1–C-1–O-4′–C-4′, Ψ = C-1–O-4′–C-4′–H-4′, ϕ = H-1–C-1–O-2′–C-2′, ψ = C-1–O-2′–C-2′–H-2′, and ω = O-5–C-5–C-6–O-6. Note that atoms with primed numbers belong to the residue closer to the reducing end in the case of Φ or Ψ and the main chain in the case of ϕ or ψ. All atoms in the definition of ω belong to the residue in the main chain. The initial dihedral conformations are set as $\Phi = 29°$, $\Psi = -30°$, $\phi = 25°$, $\psi = -35°$, and $\omega = -60°$[9,14] in which the main chain is 'flat'.

We calculated three aqueous solution systems in which the solute is a xyloglucan with the main chain restricted as flat (S_{flat}), that without restriction (S_{free}), and a cellulose oligomer without restriction (S_{cell}). In S_{flat}, we have restricted only C-1–C-4, O-5, and O-4 at glycosidic linkages in the main chain. The cellulose oligomer used in the third system is identical to the main chain of xyloglucan. Cellulose oligomers are experimentally insoluble in water when the degree of polymerization is greater than five. This calculation is thus only for reference to see the side-chain effect on the main chain in xyloglucan. Solutes are immersed in theoretical boxes with 3000 or 6000 TIP3P[19] water molecules in S_{flat} or S_{free} and S_{cell}, respectively. We performed all MD calculations using the SANDER module in the AMBER 7 program,[20] with particle mesh Ewald[21] under isothermal–isobaric periodic boundary conditions. The force-field parameter set used is the Parm99[22] augmented with the GLYCAM04[23–26] for the saccharide. Nonbonded interactions are cut off at a distance of 16 Å. The SHAKE[27] algorithm was applied to all bonds containing hydrogen atoms, consistent with the use of TIP3P waters.

Initial conjugate–gradient energy minimization was performed on all systems by using a 0.01 kcal mol^{-1} Å convergence criterion in the energy gradient. The energy minimizations were followed by a period of annealing for water with 1 fs time steps for 30 ps, during which the temperature of the system was increased and stabilized at 298 K. The initial unfavorable contacts made by the solvent were removed during the minimization and annealing, where solutes were fixed with a force constant of 200 kcal mol^{-1} Å^{-2}. After these preparations, production dynamics were performed with 2 fs time steps at 298 K and a pressure of 1 atm for 5 and 2 ns in the xyloglucan and cellulose oligomer systems, respectively. The calculation proceeded on the PCI card MD Engine II (Fuji Xerox, Tokyo) designed exclusively for MD calculations.

We used the NSOL[28] algorithm for calculation of the solvent-accessible surface area (SASA). In this algorithm, solvent is assumed as a sphere with radius R_{sol} = 1.4 Å similar to that of water, and solute atoms with radius R_{vdw}'s that are 1.9 and 1.4 Å for carbon and oxygen atoms, respectively. The solvent-accessible surface is defined as the bunch of surface of a sphere centered at a solute atom with $R_{vdw} + R_{sol}$, where the center of a spherical solvent molecule can be placed in contact with the atomic van der Waals sphere without penetrating

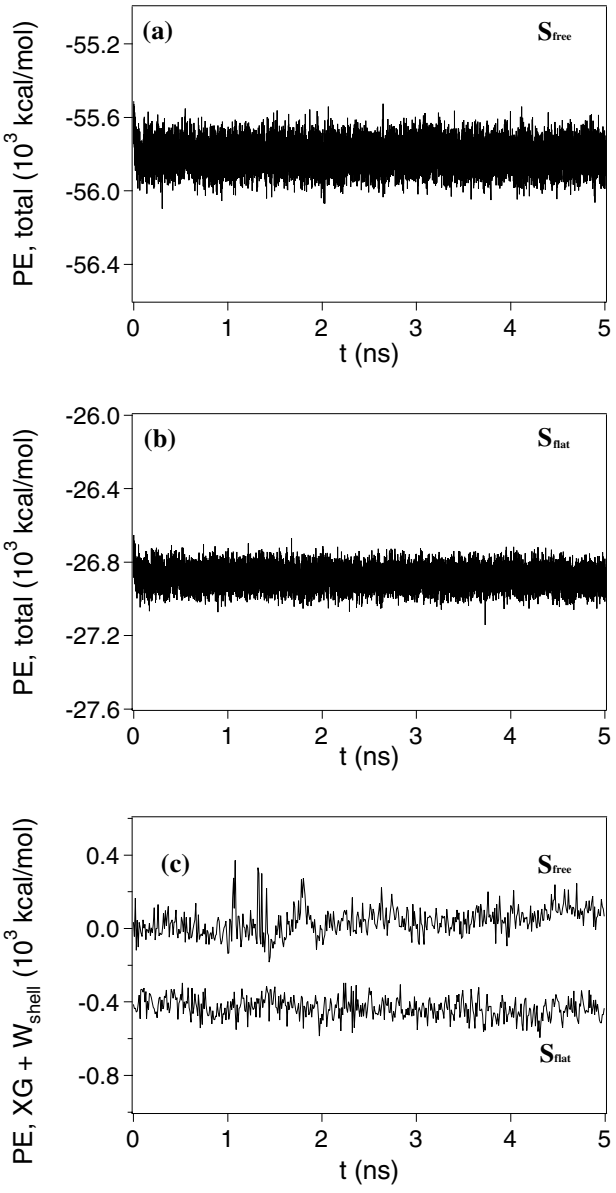

Figure 2. Plots of the potential energies (PE) throughout the trajectories. (a) The total PE of S_{free}, (b) that of S_{flat}, and (c) the PE of the xyloglucan and water molecules in close association with it in S_{free} and S_{flat}. The water molecules included for the calculation are 300 and 350 in S_{free} and S_{flat} according to the average hydration number in each system. Data are plotted per 10 ps in (c) due to limitations of the calculation procedure.

other atoms. One solvent molecule has ca. 25 Å^2 of SASA in this assumption.

3. Results and discussion

3.1. Conformational changes

The potential energies (PE's) of the systems are calculated throughout the trajectories to see the convergence of the systems (Fig. 2). As seen in Figure 2a and b, the total PE's of the systems have steady standard values after the initial declines for ca. 200 ps in both S_{free} and S_{flat}. The PE's of the xyloglucan and water molecules in close association with it are also steady in both S_{free} and S_{flat} (Fig. 2c), although some great peaks are seen in the former until 2 ns from the beginning. It is obvious that the initial unfavorable conformations of the systems are removed, and the xyloglucan is well stabilized in water within the 5-ns calculation.

We calculated the root-mean-square displacement (RMSd) of xyloglucan per atom (Fig. 3). In advance to the RMSd calculation, we fit the center of mass of xyloglucan at every step to the previous one to remove translational or rotational motions of it. The RMSd value thus depicts only the conformational changes in xyloglucan. Each system has a rapid increase of the value in the initial 200–300 ps where unfavorable conformations are removed. S_{cell} and S_{flat} reach plateaus after ca. 1 ns, although an amplitude is great in the former. S_{cell} has a standard value of ca. 6 Å after 1 ns with amplitude of ca. 4 Å. S_{free} has a maximum at ca. 2 ns with much fluctuation, and converges to ca. 8 Å after around 4 ns. When we elongate the time scale of S_{cell} twice as slowly as in S_{free}, the profile becomes similar to that in S_{free}. For example, the RMSd has the greatest value at ca. 1 and 2 ns in S_{cell} and S_{free}, respectively. The fluctuation period is approximately twice longer in S_{free} than S_{cell}, while the amplitude of fluctuation is similar. These results suggest that the side chains of the xyloglucan slow the motions of the main chain. In S_{flat}, the amplitude of fluctuation is much smaller than in the other two because of the immobilized main chain.

The conformations of xyloglucan in S_{flat} and S_{free} for the 5-ns calculation are described in Figure 4. In the initial conformation, the side chains extend obliquely up- and downward to the main-chain surface (Fig. 4a). After the 5-ns calculation, the side chains in S_{flat} tend to fold onto the main-chain surface to which the glycosidic ring faces of galactoses in the side chains are parallel (Fig. 4b). In S_{free}, the main chain takes a twisted conformation on which the side chains do not tightly fold (Fig. 4c). These conformational changes are accompanied with the xyloglucan movement of contracting and swelling. Figure 5 denotes the SASA of xyloglucan throughout the trajectory in S_{flat} and S_{free} with the most contracting conformation in the latter system. The value reaches a plateau after ca. 3 ns in S_{flat} with small movement of contracting and swelling. In S_{free}, the xyloglucan contracts most at ca. 2 ns and then turns to swell. As seen in the most contracting conformation in the figure, the contraction in S_{free} is mainly due to the embowed conformation of the main chain. In S_{free}, it has to occur entirely due to the side-chain folding, because the main

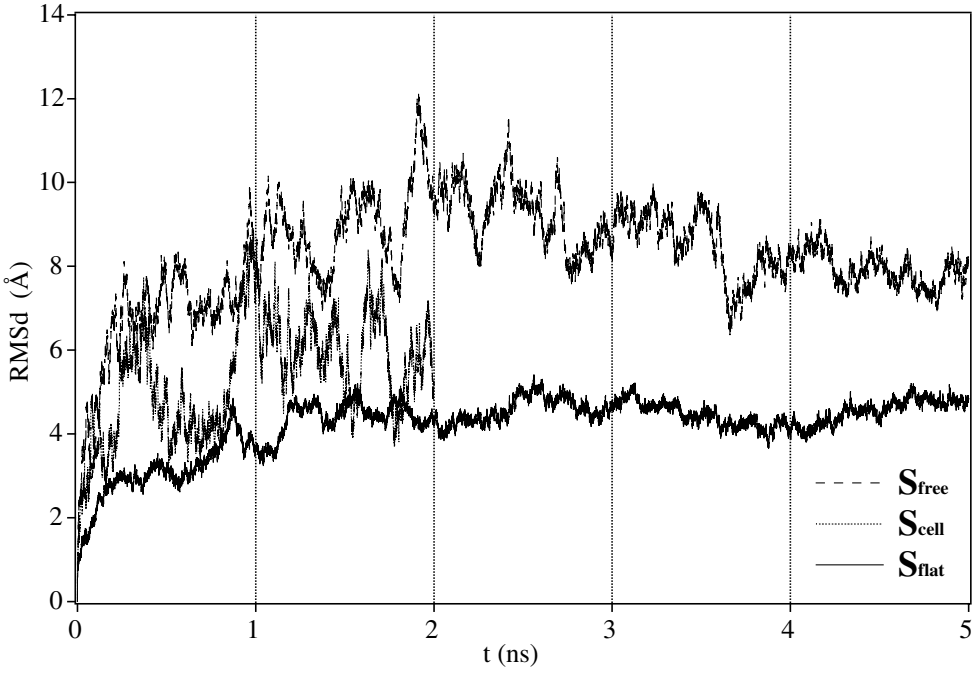

Figure 3. Root-mean-square displacement of xyloglucan per atom.

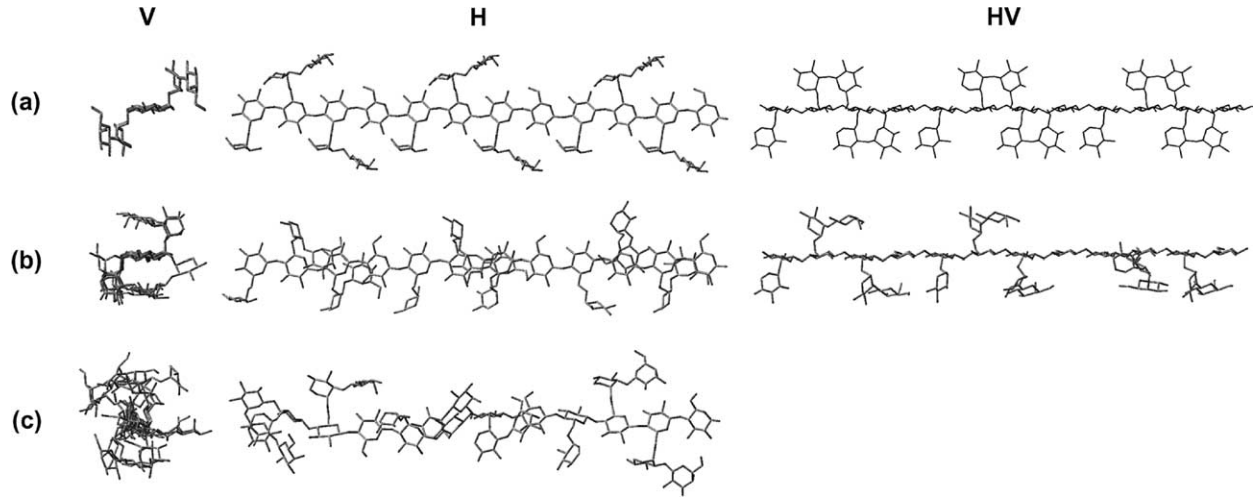

Figure 4. Xyloglucan conformation of (a) the initial, (b) average over the last 100 ps in 5-ns with the main chain restricted as flat, and (c) without restriction of the main chain. Viewed from the reducing end (V), from the above (H) and the long side of the ribbon-like surface of main chain (HV). The H and HV conformations in (c) are joined into one because the main chain is twisted.

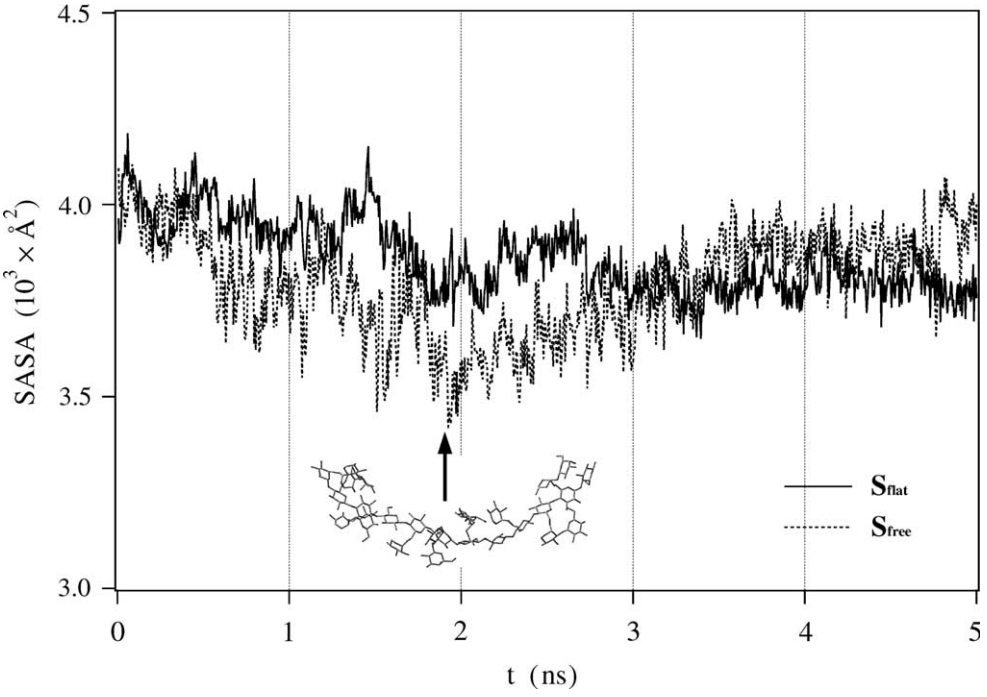

Figure 5. Solvent-accessible surface area (SASA) of xyloglucan per 5 ps in systems with the main chain restricted (solid line) and free (dashed line). The most contracted conformation in the latter system is described together.

chain cannot be twisted or embowed. The average value in the last 1 ns is slightly greater in S_{free} (3898 Å^2) than S_{flat} (3802 Å^2) over the last 100 ps; nevertheless, the main chain is twisted in the former. This indicates that the side chains fold onto the main chain more tightly in S_{flat} than S_{free}.

3.2. Dihedral angles

The deviations of dihedral angles, Φ, Ψ, and ω, from the initial conformation can well depict the motions of the main and side chains. Figure 6 denotes the sum of the deviations of every Φ and Ψ or ω throughout the trajectories. That of Φ and Ψ in S_{free} has a standard value around 500° after ca. 200 ps, denoting that the initial conformation of the main chain is well stabilized in the 5-ns calculation. The tendency of the total deviation is inversely associated with the SASA in S_{free}, denoting that the contracting/swelling motion of the xyloglucan is accompanied with the conformational change of the main chain. The total deviations of ω also reach plateaus after ca. 0.5 and 2 ns in S_{free} and S_{flat}. The deviation is greater

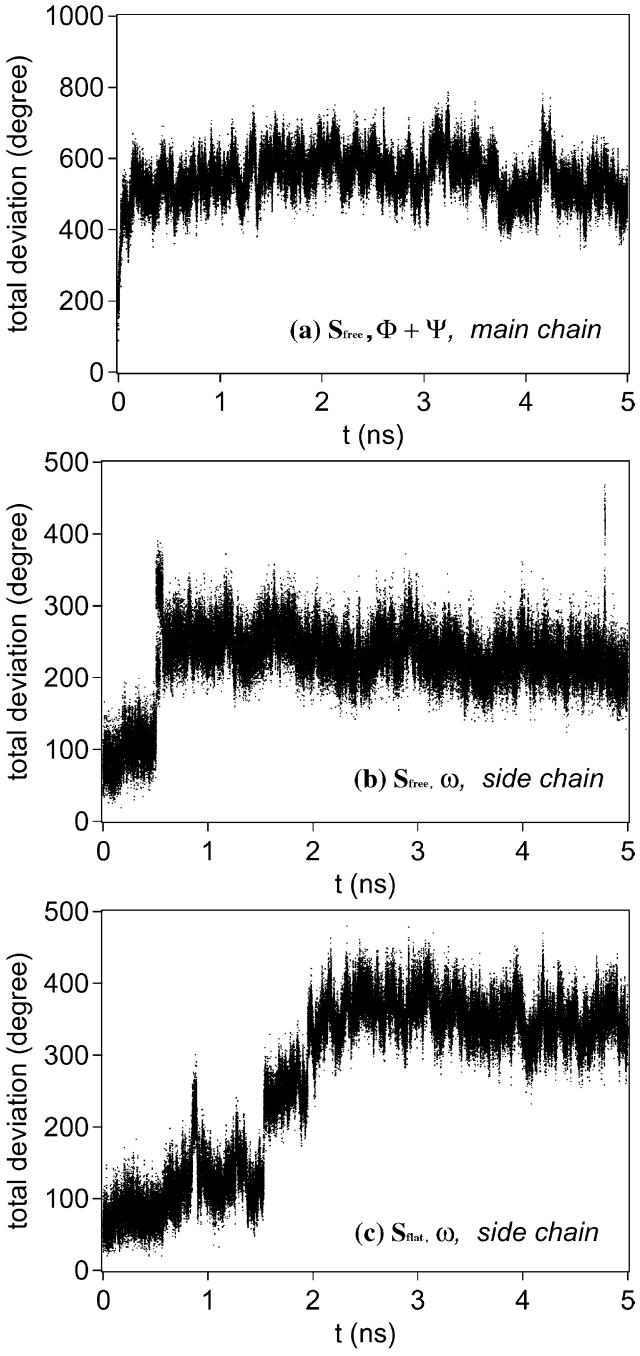

Figure 6. The total deviations of every dihedral angle of (a) Φ and Ψ in S_{free}, (b) ω in S_{free}, and (c) ω in S_{flat} from the initial configuration throughout the trajectories.

in S_{flat} (ca. 350°) than S_{free} (ca. 230°), denoting that the side chains in the former system have to change their initial conformations relative to the main chain because the main chain is restricted to be flat. As seen in Figure 4b, it is obvious that the greater deviation of ω is due to the tight folding of the side chains onto the main chain.

The distribution map of the dihedral angle pair (Φ, Ψ) enables us to grasp the twisted conformation of the main chain in S_{free} (Fig. 7). Hereafter, we use coordinate data after the initial 1 and 2 ns in cellulose and xyloglucan oligomer systems, respectively, where the initial unfavorable conformations are removed. Both the cellulose chain and the xyloglucan main chain have a maximum point of distribution at around $(\Phi, \Psi) = (45°, -5°)$. This maximum is close to the global energy minimum of cellobiose estimated in other theoretical studies,[8,11,12,14,29,30] which generates a left-handed helical conformation of cellulose backbone (Fig. 8a). We call this point a 'twisted' one. Cellobiose has another local energy minimum at around $(\Phi, \Psi) = (29°, -30°)$ in which the energy is only slightly (12 kJ mol^{-1} in Ref. 14) above the global one. This dihedral angle pair generates a 'flat,' ribbon-like conformation of the main chain that is crystalline cellulose (Fig. 8b). We call this point a 'flat' one. As seen in Figure 7a, the cellulose chain has another local maximum at around $(\Phi, \Psi) = (-25°, -30°)$ besides the twisted point on all glycosidic linkages except M8. This dihedral angle pair contributes to a reverse helical conformation, thus giving rise to the embowed conformation of the chain. We call this point an 'embowed' one. On the other hand, the xyloglucan main chain has only one maximum at the twisted point on M2, M3, M6, M8, M10, and M11 (Fig. 7b). It has another maximum at the embowed point on the other five linkages, but it is quite low on M4 and similar to those in cellulose on M7 and M9. On M1 and M5, the percentage is higher at the embowed than at the twisted point. These results mean that the xyloglucan main chain is stabilized by the side chains with less embowed conformation except on M1 and M5.

The dihedral angle ω well depicts the side chain orientation relative to the main chain (Fig. 9). The conformations are called *gg* (*gauche–gauche*) and *gt* (*gauche–trans*) when $\omega = -60°$ and 60°, respectively. As seen in Figure 9, a ring face of xylose extends vertically downward from the main-chain surface in the *gg* conformation. The conformation is similar to the *gg* one when $\omega = -90°$, but the ring face of xylose is closer to the main-chain surface. On the other hand, the xylose face is located along a side of the main-chain surface in the *gt* conformation.

The three and the two conformations of ω described in Figure 9 are major in S_{flat} and S_{free}, respectively (Fig. 10). Xylose side chains have similar distributions in S_{flat} and S_{free}; one and two of the three take the *gt* and *gg* conformations, respectively, although the former one is X1 in S_{flat} while X3 in S_{free}. A small peak at −94° in X2 is seen only in S_{flat}. On the other hand, distributions of galactose side chains show significant differences between S_{flat} and S_{free}. In S_{free}, all galactose side chains take the *gg* conformation with single-peaked distributions, although the peaks shift toward −80° at XG3 and XG4. In S_{flat}, however, the distributions at XG3, XG4, and XG6 bifurcate with peaks at around −60° and −90°. This bifurcation means that

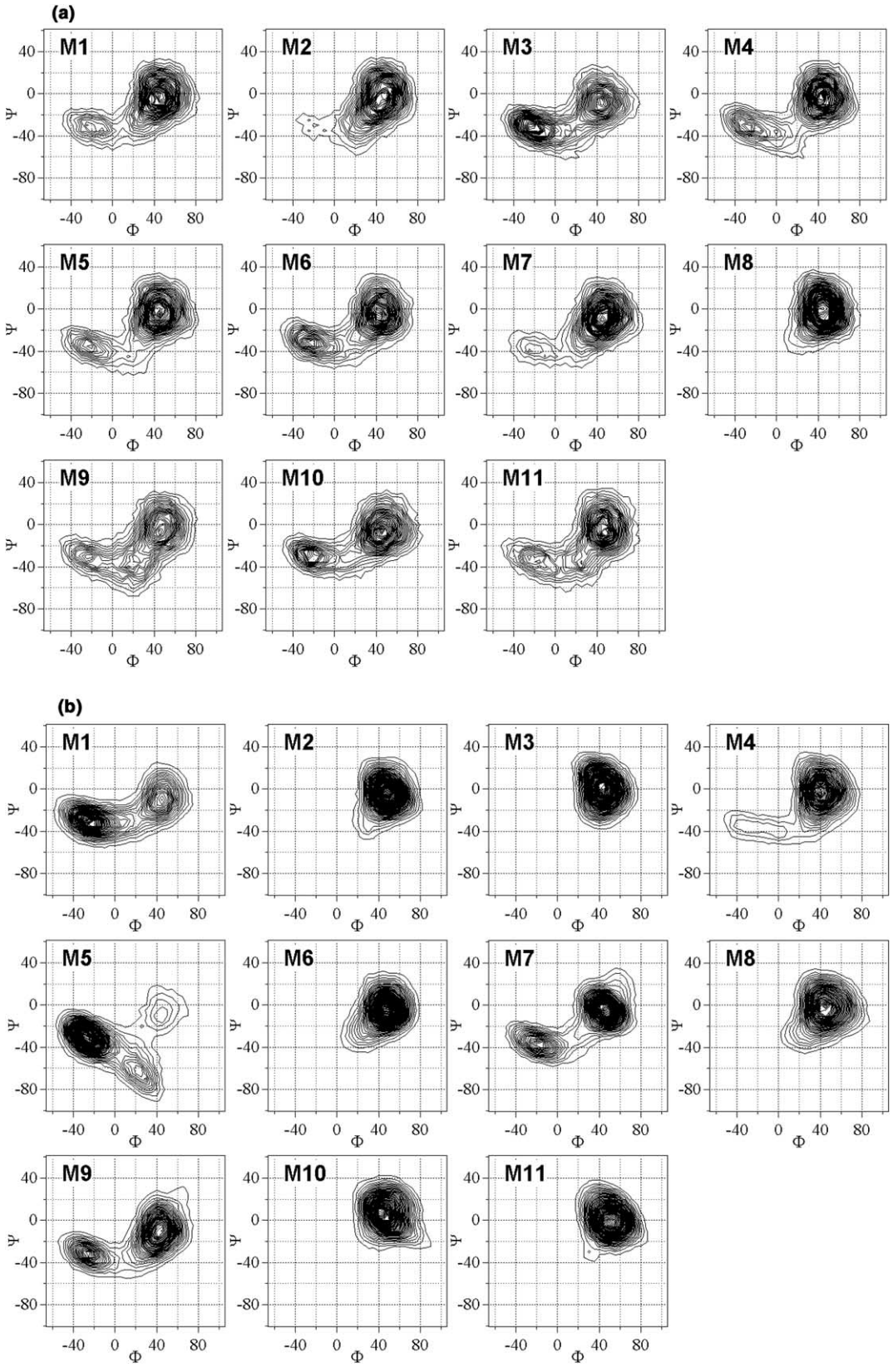

Figure 7. Distribution map of the dihedral angle pair (Φ, Ψ) as percentage over population. (a) Cellulose and (b) xyloglucan oligomers without restriction. The angle mesh unit is 5°, and the contour lines are spaced in 0.05% intervals.

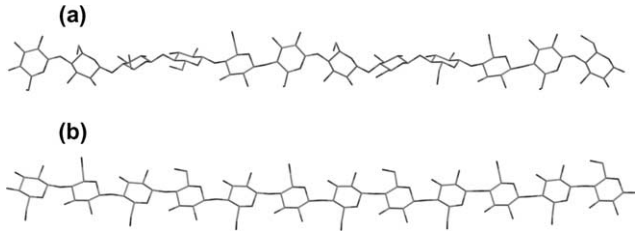

Figure 8. Representative conformations of cellulose backbone with $(\Phi, \Psi) = (a)\ (45°, -5°)$ and (b) $(29°, -30°)$.

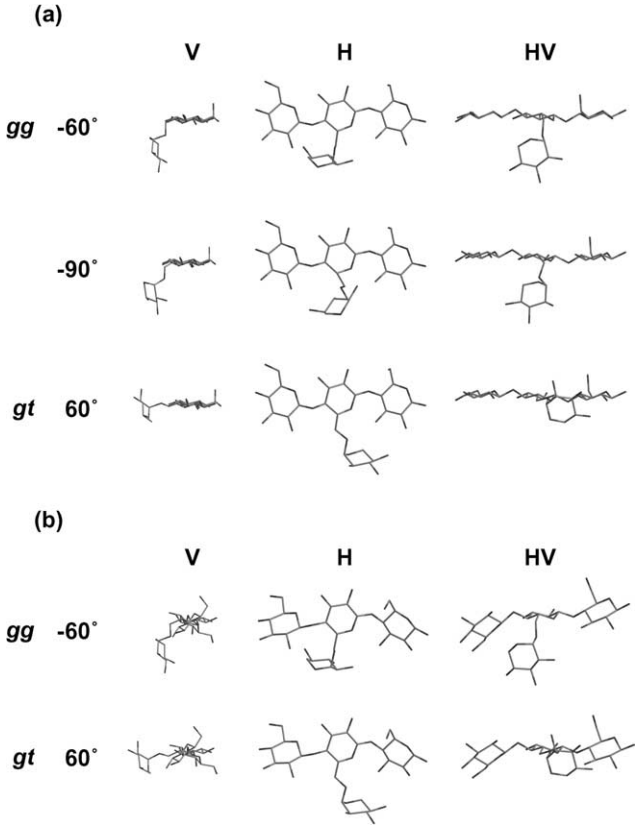

Figure 9. Side-chain orientations with $\omega = -60°$, $-90°$, and 60° to (a) flat and (b) twisted main chains. Definitions of direction V, H, and HV are the same in Figure 3. Conformations are called *gg* (*gauche–gauche*) and *gt* (*gauche–trans*) when $\omega = -60°$ and 60°, respectively.

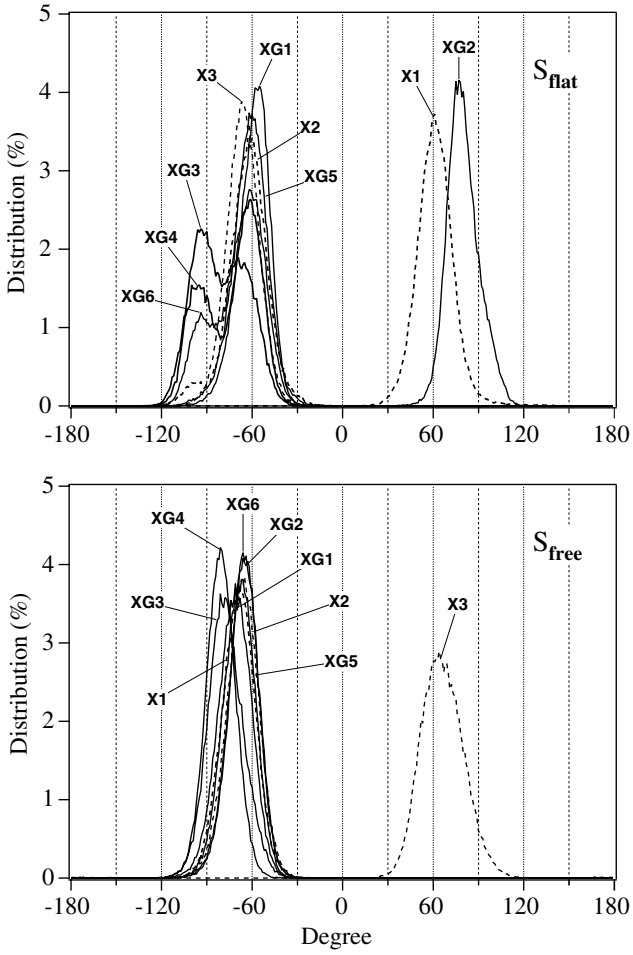

Figure 10. Distribution of the dihedral angle ω in S_{flat} and S_{free}. The solid and dashed lines denote galactose and xylose side chains, respectively.

the *gg* conformation is less stable in S_{flat} than S_{free} at the galactose side chains. In addition, XG2 takes the *gt* conformation in S_{flat}. This *gt* conformation is a result of a different positioning of galactoxylose on the main chain from the other galactoxylose side chains as mentioned later (Fig. 12a, S2). These results denote that the flat main-chain surface attracts galactose residues in a different way from the free one. It is possible that the main chain, which is restricted to be flat, attracts the side chains as close as possible to make up its conformational disadvantage to contract compared to the free one.

We show the distribution of the dihedral angle pair (ϕ, ψ) at galactose side chains S1–S6 in Figure 11. This pair distributes more widely in S_{free} than S_{flat}, denoting that the side chains have less mobility in the latter than in the former. There are at most two maxima in S_{flat}, while there are only five in S_{free}. Conformations around $(\phi, \psi) = (50°, 20°)$ and $(50°, -20°)$ are abundant in both systems. In addition to these two maxima, there is another one around $(\phi, \psi) = (15°, -50°)$ in S_{free}. In Figure 12, we draw parts of the galactose side chains with attached and adjacent glucose residues in the average structure of xyloglucan over the last 100 ps in S_{flat} and S_{free}. As seen in Table 1, the dihedral angles ω, ϕ, and ψ in the conformations are around the maximum points in Figures 10 and 11, denoting that the conformations are one of the major ones throughout the 5-ns calculation. We can see the ring face of galactose tends to parallel sticking onto the main-chain surface in S_{flat}

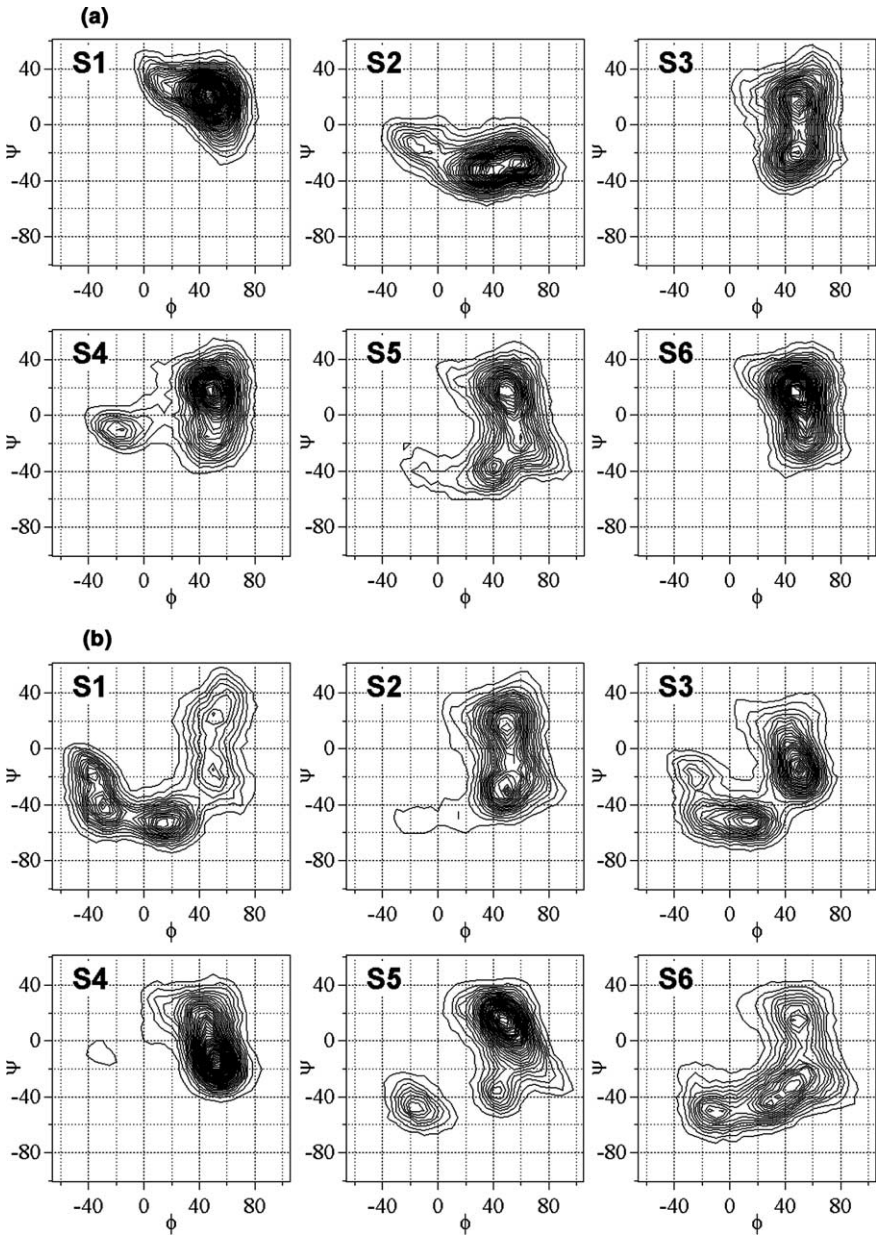

Figure 11. Distribution map of the dihedral angle pair (ϕ,ψ) as a percentage over population in (a) S_{flat} and (b) S_{free}. The angle mesh unit is 5° and the contour lines are spaced in 0.05% intervals.

(Fig. 12a). All galactose faces are below the main chain except at XG2 where the angle ω takes the *gt* conformation, unlike the others. It is considered that the galactose side chain at XG2 in S_{flat} happens to be put in the reversed position by certain interactions with other residues and water, where it has to stay due to the strong interaction between the galactose and the main-chain surface. On the other hand, all galactose residues in S_{free} extend on the diagonal to the connecting glucose (Fig. 12b). Their ring faces instead tend to be parallel to that of an adjacent glucose that is close to the reducing end (right in Fig. 12b), although the binding is moderate.

3.3. Intramolecular hydrogen bonds

The main chain of xyloglucan has a hydrophobic, ribbon-like surface and hydrophilic hydroxyl groups on its sides. To know which site of the main chain mainly interacts with the side chains, we have examined the state of intramolecular hydrogen bonds. We define a pair of an oxygen and a hydroxyl group as hydrogen bonding when (1) the two oxygens are within 3.5 Å and (2) the angle between O–H···O is from 120° to 180°.

The hydrophobic, ribbon-like surface of a cellulose oligomer or a xyloglucan main chain includes the O-5′–O-3 interresidue hydrogen bond that is very sta-

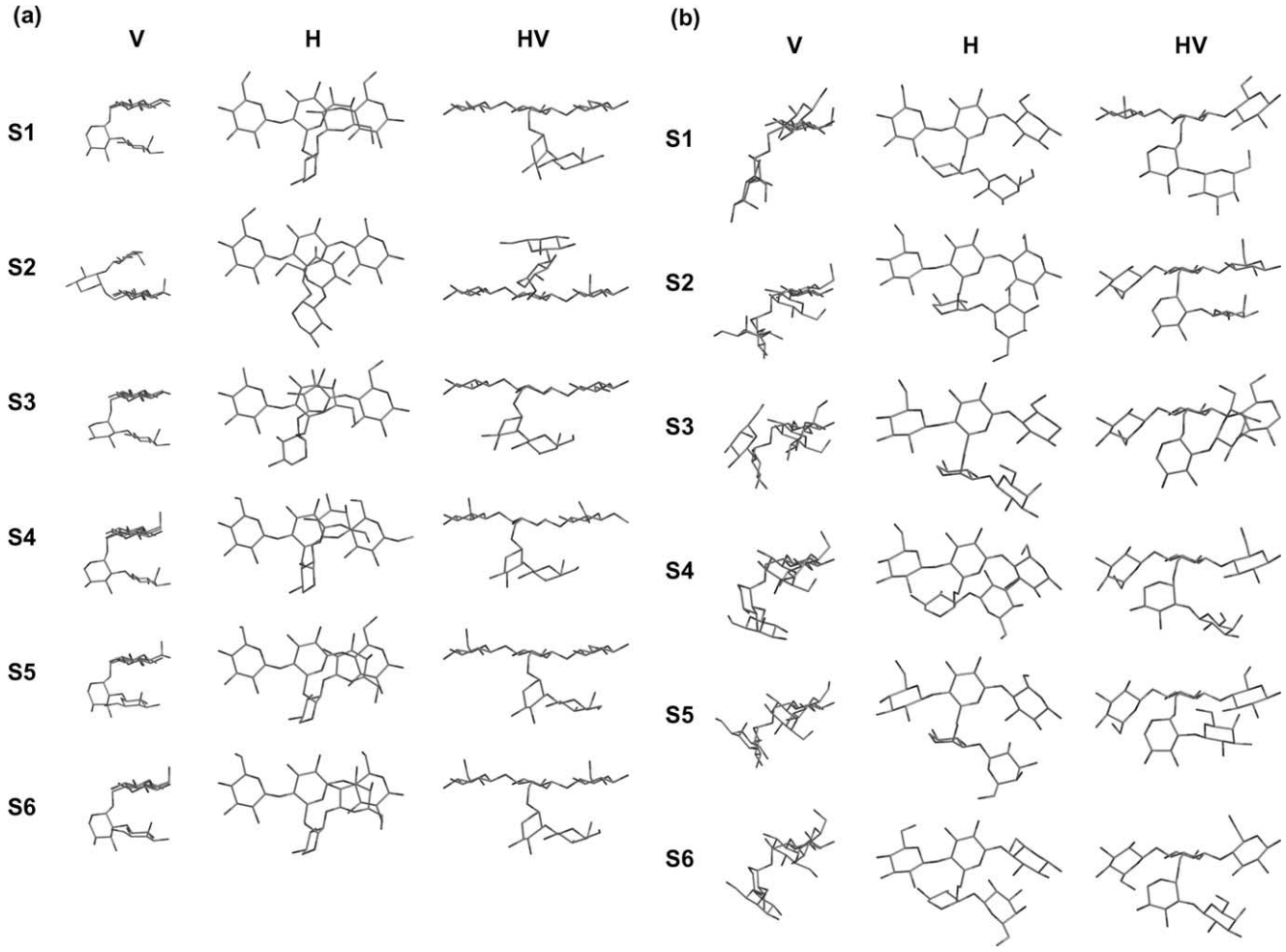

Figure 12. Conformation of the side chains at S1–S6 relative to the main chain in the average structure over the last 100 ps in (a) S_{flat} and (b) S_{free}. Definitions of direction V, H, and HV are the same in Figure 3. Each structure is aligned as the attached glucose residue takes the same direction.

Table 1. Averages and standard deviations of dihedral angles ω, ϕ, and ψ over the last 100 ps (°)

S_{flat}	Av.			Dev.		
	ω	ϕ	ψ	ω	ϕ	ψ
S1	−53	49	26	6.1	9.0	10.7
S2	83	64	−24	6.8	8.8	9.4
S3	−82	46	−8	5.6	9.6	10.5
S4	−70	48	9	8.0	8.9	11.0
S5	−59	56	23	5.7	8.2	8.3
S6	−59	50	18	6.5	8.2	11.9
S_{free}						
S1	−64	−35	−23	7.6	10.0	10.4
S2	−66	57	19	8.9	11.5	10.0
S3	−62	−2	−49	8.6	13.4	8.5
S4	−71	53	12	11.3	11.1	15.5
S5	−62	45	8	8.2	7.4	14.7
S6	−67	39	5	8.1	10.6	10.6

ble.[31,32] The occupancy of this kind of hydrogen bond is evaluated in S_{cell}, S_{flat}, and S_{free} (Table 2). It is natural that the occupancies in S_{flat} are around 80%, which is higher than the other two. In other words, the O-5′–O-3 hydrogen bond is broken when the main chain is twisted. In the 2–5 ns calculation time, the averages over M1–M11 are similar in S_{cell} (44.2%) and S_{free} (48.8%), but the standard deviations are three times greater in S_{free} (17.5%) than in S_{cell} (5.8%). This means that the twisted state of the main chain of the xyloglucan becomes inhomogeneous because the side chains stabilize the state of the main chain, as analyzed in the previous section.

When the O-5′–O-3 interresidue hydrogen bond is broken in the twisted main chain, the released O-3 or O-5 can interact with other oxygens or hydroxyl groups. To investigate destinations of the released O-3 from the O-5′–O-3 interresidue hydrogen bond, we estimate the occupancies of intramolecular hydrogen bonds at O-2, O-3, and O-6 in the main chain with ether oxygens or hydroxyl groups in side chains (Table 3). The values at the ether oxygen atoms of O-4 and O-5 in the main

Table 2. Occupancy of the O-5′–O-3 interresidue hydrogen bond in main chain (%)

Position	S_{cell}	S_{flat}				S_{free}			
	1–2 ns	2–3 ns	3–4 ns	4–5 ns	2–5 ns	2–3 ns	3–4 ns	4–5 ns	2–5 ns
M1	38.4	94.6	96.8	96.6	96.0	78.8	17.7	10.5	35.7
M2	48.3	91.4	88.4	95.1	91.6	54.3	71.2	70.8	65.4
M3	37.0	98.0	98.5	98.6	98.3	41.0	41.1	52.3	44.8
M4	43.3	70.9	73.0	84.3	76.1	55.5	45.5	36.9	46.0
M5	42.5	83.3	57.1	81.2	73.9	11.4	1.4	20.0	10.9
M6	43.1	68.0	95.3	96.3	86.6	85.6	80.1	66.5	77.4
M7	57.4	75.7	73.0	80.9	76.5	57.1	23.1	66.9	49.1
M8	47.6	71.4	78.8	82.5	77.6	42.5	49.9	53.6	48.7
M9	37.9	84.0	87.0	90.2	87.0	27.5	62.0	76.6	55.4
M10	46.5	70.1	68.2	91.6	76.6	26.4	55.6	36.8	39.6
M11	44.4	57.1	67.4	59.8	61.4	49.6	58.8	83.3	63.9
Av.	44.2	78.6	80.3	87.0	82.0	48.2	46.0	52.2	48.8
Dev.	5.8	12.7	13.8	11.2	11.0	22.0	23.8	23.6	17.5

Averages (Av.) and standard deviations (Dev.) over M1–11.

Table 3. Occupancy of intramolecular hydrogen bonds at O-2, O-3, and O-6 of main chain with side chains (%)

S_{flat}	O-2				O-3				O-6			
Residue	2–3 ns	3–4 ns	4–5 ns	2–5 ns	2–3 ns	3–4 ns	4–5 ns	2–5 ns	2–3 ns	3–4 ns	4–5 ns	2–5 ns
1	2.9	4.5	4.6	4.0	0.2	0.4	0.1	0.3	0.0	0.0	0.0	0.0
2	0.0	0.0	0.0	0.0	14.3	16.8	13.4	14.8				
3	41.9	55.1	52.8	49.9	27.0	18.3	3.0	16.1				
4	21.7	19.6	11.8	17.7	0.0	0.0	0.0	0.0				
5	0.8	1.8	0.6	1.1	0.7	0.5	1.4	0.9	0.0	0.0	0.2	0.1
6	1.5	4.0	4.9	3.8	1.3	6.3	0.3	2.6				
7	0.9	1.6	1.5	1.3	42.2	8.0	0.5	16.9				
8	1.0	0.3	0.0	0.4	0.0	0.0	0.0	0.0				
9	35.1	104.8	9.0	49.7	19.4	24.5	0.2	14.7	0.0	0.0	0.0	0.0
10	17.0	1.0	4.2	7.4	0.7	0.1	0.0	0.3				
11	27.1	2.4	0.3	9.9	1.0	12.2	0.2	4.5				
12	2.4	1.1	0.0	1.2	0.0	0.0	0.0	0.0				
Av.	12.8	16.3	7.5	12.2	8.9	7.3	1.6	5.9				0.0
Dev.	15.2	32.0	14.8	18.3	14.0	8.7	3.8	7.3				0.0
S_{free} Residue												
1	57.7	0.0	10.0	22.6	28.5	49.3	5.6	27.8	0.0	8.3	0.9	3.1
2	45.2	47.4	61.4	51.3	44.4	32.7	31.0	36.0				
3	0.1	0.2	0.0	0.1	2.0	5.8	1.1	3.0				
4	0.6	1.8	0.1	0.8	0.0	0.0	0.0	0.0				
5	2.5	0.9	17.4	6.9	0.0	2.1	32.8	11.6	8.3	3.3	2.6	4.7
6	11.1	2.9	7.8	7.3	41.4	39.1	38.8	39.8				
7	2.9	3.6	3.3	3.3	13.5	3.4	22.3	13.1				
8	0.1	3.1	0.0	1.1	0.0	0.0	0.0	0.0				
9	5.3	31.9	68.7	35.3	12.5	51.9	19.2	27.9	12.3	1.6	0.5	4.8
10	23.9	26.1	18.1	22.7	69.6	33.9	69.3	57.6				
11	0.3	16.5	17.5	11.4	9.8	42.5	8.8	20.4				
12	12.0	0.1	0.0	4.0	0.0	0.0	0.0	0.0				
Av.	13.5	11.2	17.0	13.9	18.5	21.7	19.1	19.8				4.2
Dev.	19.2	15.8	23.6	16.1	22.7	21.5	21.2	18.6				1.0

Averages (Av.) and standard deviations (Dev.) over all residues. Oxygens or hydroxyl groups in side chains are not distinguished from each other. One hydroxyl group can form more than one hydrogen bond so the percentage can be more than 100%.

chain are not described because all of them are 0%. As seen in Table 3, the average occupancies at O-2 are similar in S_{flat} (12.2%) and in S_{free} (13.9%). On the other hand, those at O-3 are more than three times higher in S_{free} (19.8%) than S_{flat} (5.9%). In S_{free}, the released O-3s from the interresidue hydrogen bond in the main

chain take part in the hydrophilic interaction between side chains instead. In addition, the occupancy of the O-5′–O-3 interresidue hydrogen bond in the main chain is only ca. 1.7 times higher in S_{flat} than S_{free} (Table 2). This means that hydrophilic interactions between the main and side chains are more abundant in S_{free} than S_{flat} because of not only the breaking of the O-5′–O-3 interresidue hydrogen bond in the main chain, but also in the twisted main chain. The occupancy at O-6 of the main chain is also higher in S_{free} while that in S_{flat} is almost 0% at every period.

As seen in the previous section, the glycosidic ring faces of galactoses in the side chains stick onto the main-chain surface in S_{flat}. The analysis of intramolecular hydrogen bonds reveals that this interaction is somewhat hydrophobic, while the interaction between the main and side chains in S_{free} is relatively hydrophilic. The folding mechanism of xyloglucan side chains onto the main chain is different in S_{flat} and S_{free}. In other words, it is revealed that the xyloglucan can control the side-chain folding by the main-chain conformation. It is possible that this ability plays a role in the gelation mechanism of a water–alcohol solution of xyloglucans. In a single system of a xyloglucan, the flat main chain attracts the side chains by intramolecular hydrophobic interaction. In a multisystem of xyloglucans, the attracting force of the flat main chain can work on the side and main chains of the other xyloglucans by intermolecular hydrophobic interaction, in addition to their own side chains. When dissolving in water, xyloglucans can lose their side-chain folding by the relatively twisted conformation of main chains. Hydrophilic interaction with water can have an influence on this loose folding because the interaction between the main and side chains of xyloglucan is relatively hydrophilic when the main chain is twisted. On the other hand, if for some reason the main chains become flat, they can attract and bind the glycosidic ring faces of other xyloglucans with hydrophobic interactions. As a result, aggregation occurs in some parts of the water–alcohol solution of xyloglucans. This may be one of the processes in gel formation. This conformational folding of side chains may also work on the cell-wall enlargement of plants because the interaction with flat cellulosic cell walls is thought to render the main chain of xyloglucan flat.

4. Conclusions

The folding mechanism of xyloglucan side chains onto the main chain depends on the condition of the main chain. When the main chain is restricted in the flat ribbon-like conformation, the glycosidic ring faces of galactose in the galactoxylose side chains stick onto the flat surface of the main chain by hydrophobic interactions. When the main chain is not restricted, it has a twisted conformation and loses the face-to-face folding of galactose on it. The flat main chain attracts the galactose side chains by a hydrophobic interaction stronger than the free and twisted one. When the main chain is not restricted, O-3s in the main chain is released from the interresidue O-5′–O-3 hydrogen bond and is able to interact with ether oxygens or hydroxyl groups in side chains with more relaxed binding.

Acknowledgments

The authors thank K. Kanayama, T. Hirotsu, and colleagues in our laboratory for useful discussions and criticism. This work is supported by the Ministry of Education, Science and Culture, Japan (support of young researchers with a term to Y.Y.).

References

1. Gibeault, D. M.; Garpita, N. C. *Plant J.* **1993**, *3*, 1–30.
2. Hayashi, T. *Ann. Rev. Plant Physiol. Plant Mol. Biol.* **1989**, *40*, 139–168.
3. Hayashi, T.; Takeda, T.; Ogawa, K.; Mitsuishi, Y. *Plant Physiol.* **1994**, *35*, 893–899.
4. Hayashi, T.; Ogawa, K.; Mitsuishi, Y. *Plant Cell Physiol.* **1994**, *35*, 1199–1205.
5. Yuguchi, Y.; Kumagai, T.; Wu, M.; Hirotsu, T.; Hosokawa, J. *Cellulose* **2004**, *11*, 203–208.
6. Yamanaka, S.; Yuguchi, Y.; Urakawa, H.; Kajiwara, K.; Shirakawa, M.; Yamatoya, K. *Food Hydrocoll.* **2000**, *14*, 125–128.
7. Yamanaka, S.; Yuguchi, Y.; Urakawa, H.; Kajiwara, K. *Sen'i Gakkaishi* **1999**, *55*, 528–532.
8. Taylor, I. E. P.; Atkins, E. D. T. *FEBS Lett.* **1985**, *181*, 300–302.
9. Ogawa, K.; Hayashi, T.; Okamura, K. *Int. J. Biol. Macromol.* **1990**, *12*, 218–222.
10. Picard, C.; Gruza, J.; Derouet, C.; Renard, C. M. G. C.; Mazeau, K.; Koca, J.; Imberty, A.; Penhoat, C. H. *Biopolymers* **2000**, *54*, 11–26.
11. Tvaroska, I. *Biopolymers* **1984**, *23*, 1951–1960.
12. Cheetham, N. W. H.; Dasgupta, P.; Ball, G. E. *Carbohydr. Res.* **2003**, *338*, 955–962.
13. Sugiyama, H.; Hisamichi, K.; Usui, T.; Sakai, K.; Ishiyama, J. J. *J. Mol. Struct.* **2000**, *556*, 173–177.
14. Levy, S.; York, W. S.; Stuike-Prill, R.; Meyer, B.; Staehelin, L. A. *Plant J.* **1991**, *1*, 195–215.
15. Levy, S.; Maclachlan, G.; Staehelin, L. A. *Plant J.* **1997**, *11*, 373–386.
16. Kooiman, P. *Recl. Trav. Chim. Pays-Bas* **1961**, *80*, 849–865.
17. White, E. V.; Rao, P. S. *J. Am. Chem. Soc.* **1953**, *75*, 2617–2619.
18. Wang, Q.; Ellis, P. R.; Ross-Murphy, S. B.; Burchard, W. *Carbohydr. Polym.* **1997**, *33*, 115–124.
19. Jorgensen, W. L.; Chandrasekhar, J.; Madura, J. D.; Impey, R. W.; Klein, M. L. *J. Chem. Phys.* **1983**, *79*, 926–935.
20. Case, D. A., Pearlman, D. A., Caldwell, J. W., Cheatham, T. E. I., Wang, J., Ross, W. S., Simmerling, C., Darden, T., Merz, K. M., Stanton, R. V., Cheng, A. AMBER 7.

University of California, San Francisco: San Francisco, CA, 2002.
21. Essmann, U.; Perera, L.; Berkowitz, M. L.; Darden, T.; Lee, H.; Pedersen, L. G. *J. Chem. Phys.* **1995**, *103*, 8577–8593.
22. Wang, J.; Cieplak, P.; Kollman, P. A. *J. Comput. Chem.* **2000**, *21*, 1049–1074.
23. Woods, R. J.; Dwek, R. A.; Edge, C. J.; Fraser-Reid, B. *J. Phys. Chem.* **1995**, *99*, 3832–3846.
24. Kirschner, K. N.; Woods, R. J. *Proc. Natl. Acad. Sci. U.S.A.* **2001**, *98*, 10541–10545.
25. Kirschner, K. N.; Woods, R. J. *J. Phys.Chem. A* **2001**, *105*, 4150–4155.
26. Basma, M.; Sundara, S.; Calgan, D.; Venali, T.; Woods, R. J. *J. Comput. Chem.* **2001**, *22*, 1125–1137.
27. Ryckaert, J. P.; Ciccotti, G.; Berendsen, H. J. C. *J. Comput. Phys.* **1977**, *23*, 327–341.
28. Masuya M. *NSOL*. http://biocomputing.cc/nsol/, 2003.
29. French, A. D.; Kelterer, A. M.; Johnson, G. P.; Dowd, M. K.; Cramer, C. J. *J. Comput. Chem.* **2001**, *22*, 65–78.
30. Hardy, B. J.; Sarko, A. *J. Comput. Chem.* **1993**, *14*, 848–857.
31. Tashiro, K.; Kobayashi, M. *Polymer* **1991**, *32*, 1516–1526.
32. Umemura, M.; Yuguchi, Y.; Hirotsu, T. *J. Mol. Struct.* (*THEOCHEM*), in press.